A New Cosine Hyperbolic Window Function-based FIR Filter design for Audio to Spectrogram Conversion

Hrishi Rakshit
Computer Science & Engineering,
School of Built Environment,
Engineering and Computing,
LEEDS BECKETT UNIVERSITY
LEEDS, UK
h.rakshit2399@student.leedsbeckett.ac.uk

Pooneh Bagheri Zadeh
Computer Science & Engineering,
School of Built Environment,
Engineering and Computing,
LEEDS BECKETT UNIVERSITY
LEEDS, UK
p.bagheri-zadeh@leedsbeckett.ac.uk

***Abstract*— In recent years, deep learning-based audio signal processing is a popular way to extract features from audio signals and make the system learnt about those extracted features and patterns. These features are used for speech recognition, tracking vehicles and different types of audio processing. In many cases, to extract salient features and make the system learnt about those features, conversion of audio signal to spectrogram is a vital step. Spectrograms exhibiting minimum noise and interference, contribute significantly to feature extraction, thereby optimizing the efficiency of the learning system. In this paper, a novel adjustable window function, based on Cosine Hyperbolic Function, is proposed to design Finite Impulse Response (FIR) low-pass filter which can be utilized for reducing noise and interference from the spectrograms. The spectral characteristics of the proposed window function are compared with the state-of-the-art window functions. The performance of the Proposed window-based FIR low-pass filter is assessed with state-of-the-art FIR low-pass filters in terms of reducing noise and interference from spectrograms. Experimental result show that the proposed window-based FIR low-pass filter outperforms the existing methods to eliminate noise and interference from audio to spectrogram conversion.**

Keywords—Main-lobe Width, Ripple Ratio, Side-lobe Roll-off ratio, Normalized Frequency response

I. INTRODUCTION

In the territory of deep learning for audio processing, the transformation of raw audio signals into spectrograms plays an important role in enhancing the model's ability to distinguish patterns and features of different classes. Spectrograms provide a visual representation of the frequency contents of an audio signal over time, encapsulating both temporal and spectral characteristics [1]. This conversion facilitates the extraction of meaningful features when Convolutional Neural Network (CNN) models are employed [1]. The utilization of spectrograms enables efficient pattern recognition, speech recognition, and sound classification [2].

On the other hand, when analysing audio signals for spectrographic representation, the window function plays a crucial role in mitigating spectral leakage and minimizing the effect of extraneous noise [3]. By segmenting the signals into overlapping frames and applying a window function, the Finite Impulse Response (FIR) filter effectively reduces abrupt transitions at the frame's boundaries, preventing spectral leakage that could amplify noise components [4]. The tapper edges of window function contribute to smoother signal transition, isolating the relevant signal components and suppressing the influence of unwanted noise in the frequency domain. Thus, involving window-based FIR filter improves the precision of the spectrogram analysis and serves as an effective means of enhancing Signal to Noise Ratio (SNR) and Signal to Interference Ratio (SIR) in audio processing applications [5].

The impulse response of an ideal filter is inherently infinite, presenting a challenge in practical implementations. A conventional approach to address this issue involves rendering the response finite by truncating the ideal response. In engineering aspect, this process is done by multiplying of the ideal response $h_d(n)$, with a finite window function, typically represented by w(n). Windows, in this context, are finite arrays characterized by coefficients strategically designed to meet specific criteria and fulfil engineering requirements [6]. In general window function can be defined as equation (1).

$$W(n) = \begin{cases} f(n), & 0 \le n \le N \\ 0, & otherwise \end{cases} \quad (1)$$

Where n=number of samples and N=order of the filter. The impulse response of the system is given by as equation (2).

$$h(n) = h_d(n)w(n) \quad (2)$$

The critical spectral attributes of a window function that comprise three primary characteristics are: i) the Main-lobe Width, ii) the Ripple Ratio and iii) the Side-lobe Roll-off Ratio. A higher Side-lobe Roll-off Ratio means, the filter has the capability to reject the far end interference [7]. In the realm of filter design application, this characteristic proves advantageous by minimizing attenuation in the far end spectrum [8]. Furthermore, within the domain of speech processing, a superior side-lobe roll-off ratio serves the purposes of reducing energy leakage across distinct frequency bands [9]. Hence, a window-based filter with an elevated side-lobe roll-off ratio will generate spectrograms for audio sounds characterized by diminished noise levels and rendering the training process of CNN models more efficient.

II. SPECTRAL PROPERTIES OF WINDOWS

The efficiency of a window function centres primarily on its spectral characteristics, specially the Main-lobe Width (W_M), the Ripple Ratio (R) and the Side-lobe Roll-off Ratio (S) as delineated as Fig. 1.

$$W_R = \frac{1}{2} \times \textit{the Mainlobe width}$$

$$W_M = 2 \times W_R$$

$$R = (\textit{Maximum sidelobe amplitude in dB}) - (\textit{Mainlobe amplitude in dB})$$

$$S = (\textit{Max. sidelobe amplitude in dB}) - (\textit{Min. sidelobe amplitude in dB}) = S1 - SN$$

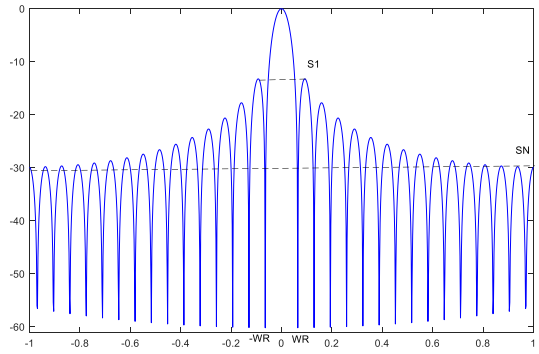

Fig. 1: A typical window's normalized amplitude spectrum

A narrower main-lobe width means a more focused frequency response, while a wider main-lobe width may lead to indicate spectral leakage and reduced frequency resolution [10]. A lower ripple ratio denotes reduced oscillation within the main-lobe width, contributing to a more stable and predictable frequency response [11]. A higher side-lobe roll-off ratio signifies a faster decrease in amplitude, minimizing interference from side lobes and improving the selectivity of the window [11].

III. The Proposed Window Function

A novel window function is proposed for converting audio sounds to spectrograms. The mathematical, expression of the proposed window function is given by as equation (3).

$$w = 0.5 - 0.5cosh\left[\sigma sin\left\{\pi \frac{\left(n-\frac{N-1}{2}\right)}{N-1}\right\}\right] \quad (3)$$

Investigation of Fig. 2 exposes that the Proposed window displays as a bell-shaped form, exemplified by a main-lobe width of 2π×0.1174 rad/sample, a ripple ratio of -31.04 dB and the side-lobe roll-off ratio of 66.18dB. These parameters were monitored with a window length of 35 and a tuning parameter of σ=0.5. Controlling the tuning parameter facilitates the generation of various window shapes and their respective normalized frequency responses as depicted in Fig. 3 and Fig. 4.

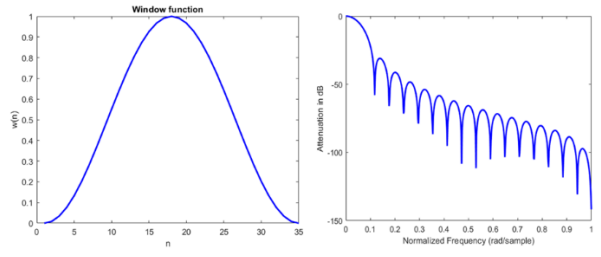

Fig. 2: The Proposed window function with normalized frequency response, N=35 and σ=0.5

Fig. 3 illustrates the different window shapes at different values of σ, when the length of the window is fixed to 256. When σ is set to 0.0000001, the resultant window shape demonstrates a sawtooth pattern. In contrast, for σ values of 0.0005 and 1, the window adopts a bell-shaped configuration. Moreover, the upper position of the window gets flattened when the values of σ are increased to 10 and 30, and approaching a shape closely resembling a rectangular window.

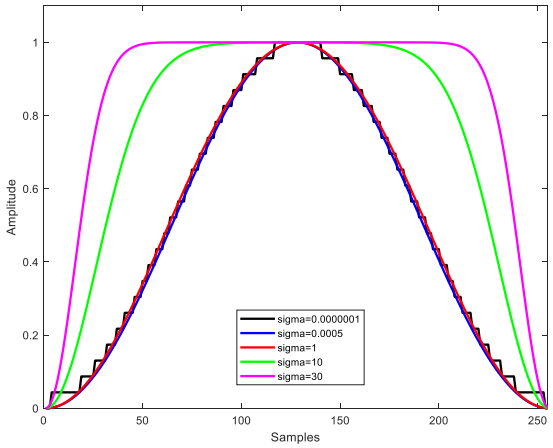

Fig. 3: Proposed window with different values of σ, when window length is fixed to 256

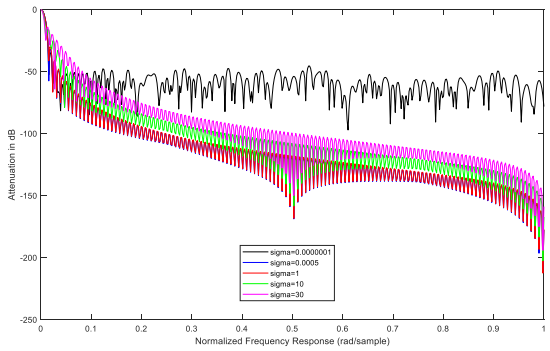

Fig. 4: Normalized frequency response of the proposed window at different values of σ when the window length is fixed to 256

TABLE I. Relationship among the Controlling Parameter (σ), Main-lobe Width (W_M), Ripple Ratio (R) and the Side-lobe Roll-off Ratio (S)

Controlling Parameter (σ)	Main-lobe Width (W_M) rad/sample	Ripple Ratio (R) dB	Side-lobe Roll-off Ratio (S) dB
0.0000001	2π×0.0157	-35.0595	22.7454
0.0005	2π×0.0157	-32.1941	130.5719
1	2π×0.0157	-30.8741	131.3409
10	2π×0.0098	-16.4381	136.9219
30	2π×0.0098	-14.1677	130.6033

Fig. 4 sketches the normalized frequency response of the proposed window at varying values of σ, as maintaining a fixed window length of 256. For σ = 0.0000001, the main-lobe width is 2π×0.0157 rad/sample, the ripple ratio is -35.0595 dB and the side-lobe roll-off ratio is 22.7454 dB. With the increment of the σ, the main-lobe width decreases while both the ripple ratio and the side-lobe roll-off ratio increases. The

most substantial findings including the narrowest main-lobe width, the utmost ripple ration and the highest side-lobe roll-off ratio, were noted at σ =30. Specifically, the main-lobe width reached a value of 2π×0.0098 rad/sample, the ripple ratio touched at -14.1677 dB and the side-lobe roll-off ratio pointed at 130.6033 dB. Table I provides a summary of the findings.

IV. Proposed Window Vs State-of-the-Art Windows

This section directs a comparative analysis of the shape and the spectral characteristics of the Proposed window together with commonly used State-of-the-Art window functions.

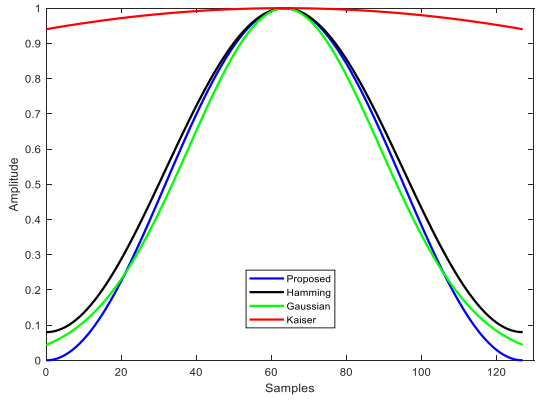

Fig. 5: Time domain representation of the Proposed and State-of-the-Art windows with window length of 128

Hamming window function is widely used in different aspects of signal processing. One of its defining features is the moderate roll-ff of side-lobes, making it a balanced choice for various applications. Hamming window is particularly used where a compromise between the main-lobe width and ripple ratio is desirable [12]. Mathematically, it can be expressed as equation (4).

$$w = 0.54 - 0.42\cos\left(\frac{2n\pi}{N}\right) \quad (4)$$

Where the window length is N+1.

Gaussian window derived from Gaussian distribution. This window function is characterized by a symmetric bell-shaped curve that gradually tapers towards the edges. The defining feature of the Gaussian window is its exceptional side-lobe suppression, minimizing spectral leakage and offering a superior level of precision in frequency analysis [10]. The mathematical expression of Gaussian window function is given by as equation (5).

$$w = e^{-\frac{1}{2}\left(\frac{\alpha n}{N/2}\right)^2} \quad (5)$$

The Kaiser window is very versatile and widely employed window function in signal processing. Its tuneable parameter enables precise control over its spectral properties. The kaiser window is characterized by its ability to adapt to specific application requirements through the adjustment of a shape parameter, often denoted as β [11]. Mathematically, Kaiser window function can be denoted as equation (6).

$$w = \frac{I_0\left(\pi\beta\sqrt{1-\left(\frac{2n}{N-1}-1\right)^2}\right)}{I_0\left(\pi\beta\right)} \quad (6)$$

Where I_0 the zeroth order modified Bessel function of first kind.

From Fig. 5, it is clear that, the Proposed window has narrower temporal compared to Hamming window. The shape of the proposed window is very similar to the gaussian window with the exception that all the coefficients of the Gaussian window is greater than zero, while the proposed window touches the X-axis in a symmetric manner. The Kaiser window with its tuneable parameter β=0.5, is almost like rectangular window with window length of 128. On the contrary, the proposed window with controlling parameter of σ=0.5, is a bell-shaped window when the window length is set to 128.

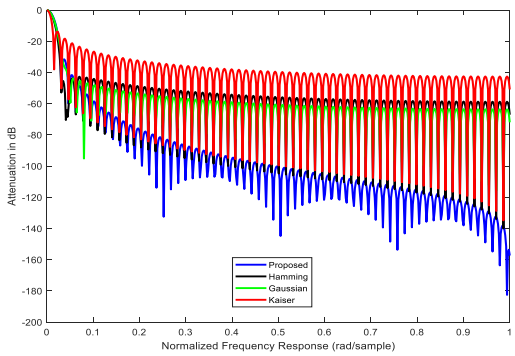

Fig 6: Normalized frequency response comparison of the Proposed window and the State-of-Art windows

Fig. 6 represents the normalized frequency responses of the Proposed and State-of-the-Art windows. In comparing windows with equal main-lobe widths and a bit higher ripple ratio, the Proposed window beats the Hamming window by 108.1362 dB in side-lobe roll-off ratio, indicating superior selectivity in passing bands and thus helps to reduce noise and interference. In contract to the Gaussian window, the Proposed window shows distinct spectral characteristics with same window length of 128, featuring a narrower main-lobe width of 2π×0.0313 rad/sample, a ripple ratio of -32.0908 dB and a considerably higher side-lobe roll-off ratio of 121.44 dB highlighting its dominance in frequency selectivity and noise reduction. The Proposed window outperforms the Kaiser window with a lower ripple ratio of -33.9778 dB and a higher side-lobe roll-off ratio of 121.2232 dB. Thus, the Proposed window demonstrates its capability in noise and interference reduction when compared to State-of-the-Art windows.

V. FIR Filter Design and Performance Evaluation

This section addresses the application of the proposed window in designing of a FIR low-pass filter, along with a comparative analysis of simulation results with widely used windows. Having a cut-off frequency of ω_c, the impulse response of an ideal low-pass filter is given by as the equation (7).

$$h_{Lp,ideal}[n] = \frac{\sin\left(\omega_c n\right)}{\pi n} \quad (7)$$

By windowing this Infinite Impulse Response (IIR) filter with the windows discussed here, different FIR filter can be achieved.

A. Proposed Window-based FIR filter

If the equation (7) is windowed by the proposed window function, the proposed window-based FIR filter is attained.

The spectral properties of the Proposed window-based FIR filter are influenced by both the controlling parameter and the order of the filter.

Fig. 7 describes the relationship between main-lobe width and the order of the Proposed filter at different vales of controlling parameter. An increment in the controlling parameter results in a reduction in the main-lobe width, maintaining a constant filter order. On the other hand, with the increment of the filter order, the main-lobe width decreases exponentially when the controlling parameter is fixed. The specific numerical values correspond to this analysis are provided in Table II.

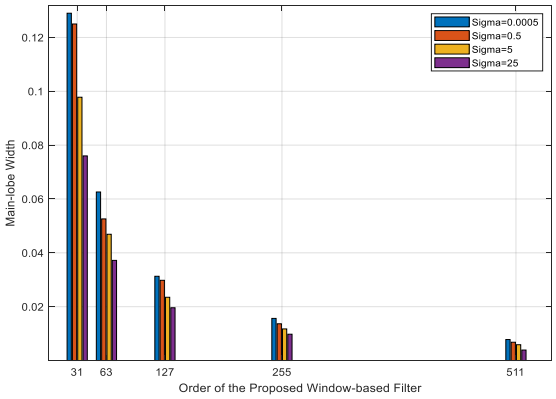

Fig. 7: Relationship between Main-lobe width and Order of the Proposed window-based filter at different values of controlling parameter

TABLE II. MAIN-LOBE WIDTH VS CONTROLLING PARAMETER AT DIFFERENT FILTER ORDERS

C. Parameter	**Main-lobe Width at different values of Proposed Filter's order**				
σ	***N=31***	***N=63***	***N=127***	***N=255***	***N=511***
0.0005	2π×0.129	2π×0.0626	2π×0.0313	2π×0.01565	2π×0.0078
0.5	2π×0.125	2π×0.0526	2π×0.0298	2π×0.01365	2π×0.0068
5	2π×0.0978	2π×0.0469	2π×0.0235	2π×0.01174	2π×0.00587
25	2π×0.076	2π×0.0372	2π×0.0196	2π×0.00978	2π×0.0039

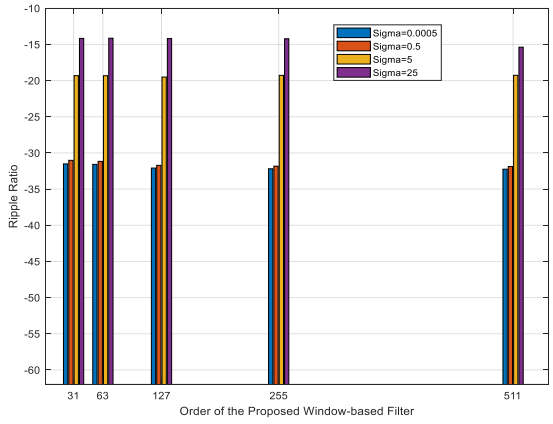

Fig. 8: Relationship between Ripple Ratio and Order of the Proposed window-based filter at different values of controlling parameter

Fig. 8 and Table III express the correlation between the Ripple Ratio and the order of the Proposed filter at different vales of controlling parameter. It has been observed that with the increment of the value of the controlling parameter, the ripple ratio increases when the filter order is fixed. Conversely, when altering the filter order while keeping the controlling parameter constant, the ripple ratio results relatively consistent values. Numeric values of Fig. 8 are expressed in Table III.

Fig. 9 and Table IV convey the association between Side-lobe Roll-off Ratio and the order of the Proposed filter at different vales of controlling parameter. As the order of the filter increases, the side-lobe roll-off ration also increases when σ remains constant.

TABLE III. RIPPLE RATIO VS CONTROLLING PARAMETER AT DIFFERENT VALUES OF FILTER ORDER

C. Parameter	**Ripple Ratio at different values of Proposed Filter's order**				
σ	***N=31***	***N=63***	***N=127***	***N=255***	***N=511***
0.0005	-31.517	-31.584	-32.0908	-32.194	-32.2486
0.5	-31.025	-31.167	-31.72	-31.83	-31.88
5	-19.32	-19.328	-19.508	-19.28	-19.27
25	-14.167	-14.142	-14.19	-14.22	-15.38

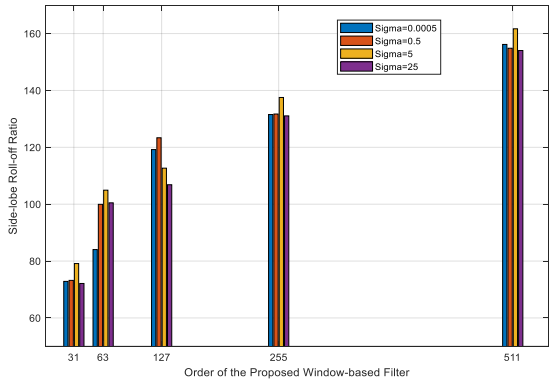

Fig 9: Relationship between Side-lobe Roll-off Ratio and Order of the Proposed window-based filter at different values of controlling parameter

In contrast, varying σ, while maintaining a constant filter order, yields a diverse pattern in the side-lobe roll-off ratio. With filter order 31, 63, 255 and 511, the highest side-lobe roll-off ratio achieve for σ=5. For the filter order 127, the maximum side-lobe roll-off ratio occurs, when σ= 0.5.

TABLE IV. SIDE-LOBE ROLL-OFF RATIO VS CONTROLLING PARAMETER AT DIFFERENT VALUES OF FILTER ORDER

C. Parameter	**Side-lobe Roll-off Ratio at different values of Proposed Filter's order**				
σ	***N=31***	***N=63***	***N=127***	***N=255***	***N=511***
0.0005	72.85	84.042	119.207	131.529	156.186
0.5	73.21	99.95	123.359	131.712	154.848
5	79.12	104.93	112.67	137.533	161.68
25	72.12	100.48	106.84	131.054	154.041

B. *Proposed Window-based filter Vs Hamming Window-based filter*

Fig. 10 and Table V express the normalized frequency response of FIR low-pass filter designed by using the Proposed and the Hamming window functions with same order of the filters. It has been observed that with same cut-off frequency, the Proposed window-based FIR Low-pass filter results 4.638 dB and 90.7482 dB better ripple ratio and side-lobe roll-off ratio respectively than the Hamming window-based FIR low-pass filter.

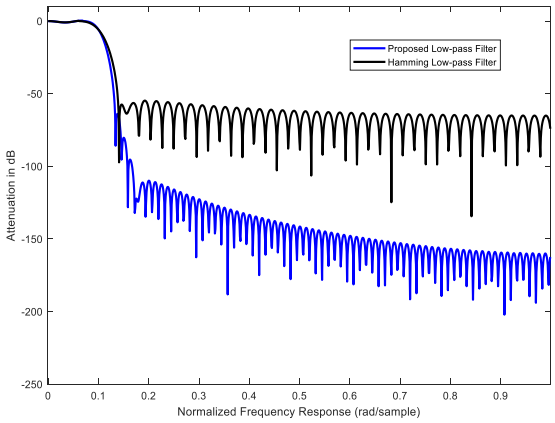

Fig. 10: Normalized frequency response of FIR low-pass filter designed by the Proposed and the Hamming window functions

TABLE V. SPECTRAL PERFORMANCE MEASUREMENT BETWEEN THE PROPOSED AND THE HAMMING WINDOW-BASED FIR LOW-PASS FILTERS

Comparing Windows	Main-lobe Width (rad/sample)	Ripple Ratio (dB)	Side-lobe Roll-off Ratio (dB)
Proposed	2π×0.1339	-62.5363	97.9317
Hamming	2π×0.1408	-57.8983	7.1835

C. *Proposed Window-based filter Vs Kaiser Window-based filter*

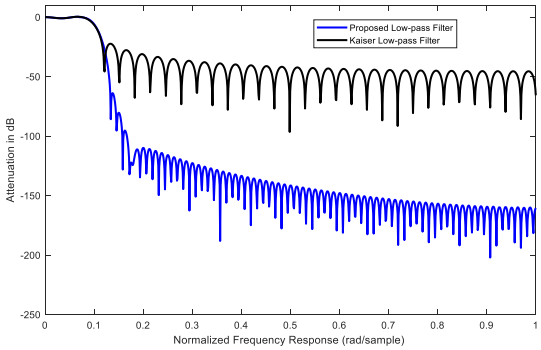

Fig. 11: Normalized frequency response of FIR low-pass filter designed by the Proposed and the Kaiser window functions

TABLE VI. SPECTRAL PERFORMANCE MEASUREMENT BETWEEN THE PROPOSED AND THE KAISER WINDOW-BASED FIR LOW-PASS FILTERS

Comparing Windows	Main-lobe Width (rad/sample)	Ripple Ratio (dB)	Side-lobe Roll-off Ratio (dB)
Proposed	2π×0.1339	-62.5363	97.9317
Kaiser	2π×0.1212	-22.9632	22.7183

The normalized frequency response of FIR low-pass filters designed by the Proposed and the Kaiser window functions are exhibited in Fig. 11 and Table VI with identical order of the filters. The Proposed window-based low-pass filter results 39.57 dB improved ripple ratio and 75.2134 dB better side-lobe roll-off ratio compared to the Kaiser window-based low-pass filter with same cut-off frequency.

D. *Proposed Window-based filter Vs Gaussian Window-based filter*

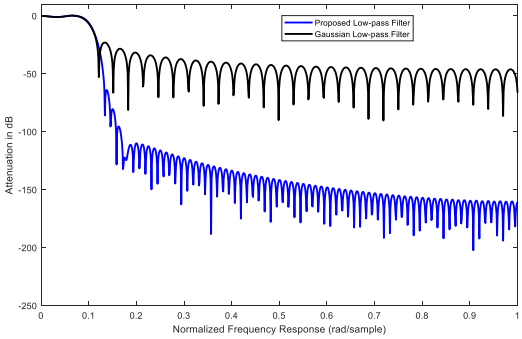

Fig. 12: Normalized frequency response of FIR low-pass filter designed by the Proposed and the Gaussian window functions

TABLE VII. SPECTRAL PERFORMANCE MEASUREMENT BETWEEN THE PROPOSED AND THE GAUSSIAN WINDOW-BASED FIR LOW-PASS FILTERS

Comparing Windows	Main-lobe Width (rad/sample)	Ripple Ratio (dB)	Side-lobe Roll-off Ratio (dB)
Proposed	2π×0.1339	-62.5363	97.9317
Gaussian	2π×0.1212	-23.0395	23.0524

Fig. 12 and Table VII show the normalized frequency response of FIR low-pass filter designed by the Proposed and the Gaussian window functions. Under equivalent conditions of cut-off frequency and filter order, the Proposed low-pass filter attains 39.5 dB and 74.8793 dB better ripple ratio and side-lobe roll-off ratio respectively compared to the Gaussian window-based low-pass filter.

The Proposed filter exhibits exceptional performance in side-lobe roll-off ratio and ripple ratio calculations, demonstrating its efficacy in noise reduction for audio signals. However, it's transition band lacks the sharpness required for processing very small Bio-signals effectively. Consequently, the Proposed filter may not be the optimal choice for applications involving such minute Bio-signals.

VI. AUDIO TO SPECTROGRAM CONVERSION

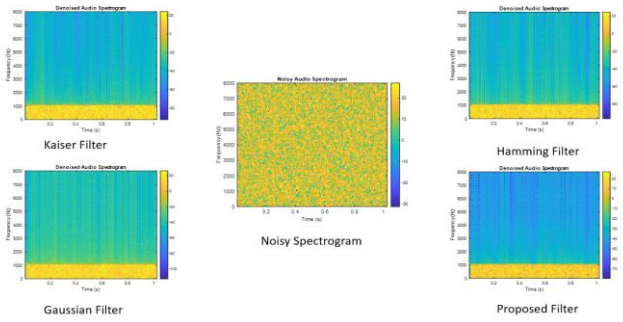

Fig. 13a: Performance comparison among the state-of-arts windows and the proposed window-based filters for denoising spectrogram in terms of colour

In the presented analysis, the spectrograms of noisy audio exhibit a distinct greenish yellow hue whereas the signal spectrograms are depicted in blue. Thus, a denoised spectrogram closely resembling the blue hue, suggests effective noise reduction. Observation of Fig.13a reveals that while the Kaiser filter shows discernment between noise and signal, residual noise persists, evident from scattered greenish yellow hues in the denoised spectrogram. Similarly, the Spectrogram achieved from the Hamming filter, presents residual scattered noise. Notably, the Gaussian filter results a predominant scattering of noise in the denoised spectrogram. Conversely, the spectrogram obtained from the Proposed Filtering method, closely resemble the blue hue, indicating more precise noise reduction compared to the State-of-Art window based filters. While assessing filter performance based on spectrogram colour may not always be optimal solution, evaluating Signal to Noise Ratio (SNR) and Signal to Interference Ratio (SIR) provide more reliable measure.

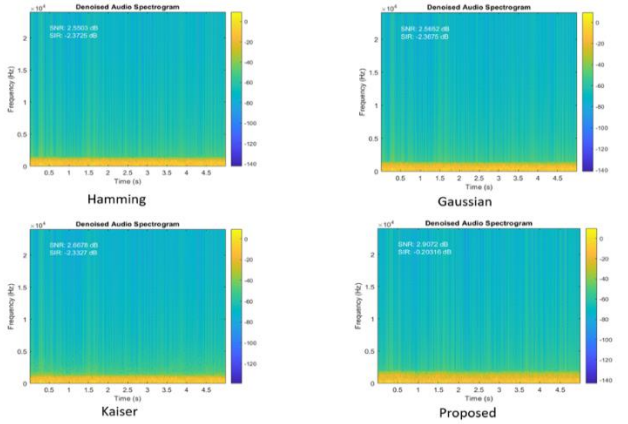

Fig 13b: Performance comparison among the state-of-arts windows and the proposed window-based filters for denoising spectrogram in terms of SNR and SIR measurement

Fig. 13b shows the denoised audio spectrogram of an audio file using various state-of-the-art window-based filters and the Proposed window-based filter with cut-off frequency of 1KHz and filter order of 256. Here Signal to Noise Ratio (SNR) and Signal to Interference Ratio (SIR) are measured to evaluate the performance of the filters. SNR of the Hamming, the Gaussian and the Kaiser filters are 2.5503 dB, 2.5652 dB and 2.6678 dB, respectively. On the other-hand, SNR of the Proposed window-based filter is 2.9072 dB which is 0.2394 dB better than the best performing Kaiser filter. The Hamming, the Gaussian, and the Kaiser filters achieve SIR of -2.3725 dB, -2.3675 dB and -2.3327 dB, respectively. The Proposed window-base filter has the SIR of -0.208316 dB which tops the performance of the state-of-art filters.

VII. Conclusion

This paper represents a novel adjustable window function which is used to design FIR low-pass filter for reducing noise from spectrograms. The Proposed window has the highest Side-lobe Roll-off Ratio compared to the most commonly used window functions like the Hamming, the Kaiser and the Gaussian window functions. The Proposed window-based FIR low-pass filter also exhibits the highest ripple ratio and side-lobe roll of ratio compared to the Hamming, the Kaiser and the Gaussian window-based FIR low-pass filters. It is clear from the experimental results that the Proposed window-based FIR low-pass filter has the ability to reduce noise and interference more precisely than the existing techniques, and thus helps to extract more accurate and details features from spectrogram images. In future, this novel Cosine Hyperbolic window-based FIR Low-pass filter, could be utilized for reducing noise from RGB images.

References

[1] Lonce Wyse, “Audio spectrogram representations for processing with Convolutional Neural Networks”, arXiv:1706.09559v1 [cs.SD] 29 Jun 2017.

[2] Anusha, N. and Roy, L, “Object Tracking from Audio and Video data using Linear Prediction method”, National Institute of Technology, Rourkela Master’s thesis. May 2015.

[3] Md Abdus Samad “A Novel Window Function Yielding Suppressed Main-lobe Width and Minimum Side-lobe Peak”, International Journal of Computer Science, Engineering and Information technology (IJCSEIT), Vol 2, No 2, April 2012.

[4] Rikita Gohil, “Design and Realization of Digital Filter”, INTERNATIONAL JOURNAL OF CREATIVE RESEARCH THOUGHTS - IJCRT (IJCRT.ORG), Volume 10, Issue 11 November 2022 ,ISSN: 2320-2882.

[5] R. Avanzato, F. Beritelli, G. Capizzi, and G. Lo Sciuto, “A new design methodology for window-based FIRfilters”, Electronics Letters, Volume 59, Issue 11, Jun 2023.

[6] Hrishi Rakshit and Muhammad Ahsan Ullah “A Comparative Study on Window Functions for Designing Efficient FIR Filter”. In Proceedings of the IEEE 9th International Forum on Strategic Technology (IFOST), ISBN: 978-1-4799-6060-6 DOI: 10.1109/IFOST.2014.6991079 pp 91-96, 2014.

[7] Bergen SWA, Antoniou A, “Design of ultraspherical window functions with prescribed spectral characteristics”,EURASIP J Appl Signal Process 2004;13:2053–65.

[8] Ibrahim Abdulhadi Sulaiman, Hussain Mohammad Hassan, Mohammad Danish, Munendra Singh, P.K. Singh, and Manisha Rajoriya, “Design, comparison and analysis of low pass FIR filter using window techniques method”, Materials Today, Volume 49, Part 8, 2022, Pages 3117-3121.

[9] Suman Yadav, Manjeet Kumar, Richa Yadav and Ashwini Kumar, “A novel approach to design optimal digital FIR filter based on logistic distribution based approximation”, International Journal of Electronics, Volume 110, Issue 3, 2023.

[10] Hrishi Rakshit and Muhammad Ahsan Ullah, “A New Efficient Approach for Designing FIR Low-pass Filter and Its Application on ECG Signal for Removal of AWGN Noise”, IAENG International Journal of Computer Science, 43:2, IJCS_43_2_05.

[11] Hrishi Rakshit and Muhammad Ahsan Ullah, “FIR Filter Design Using An Adjustable Novel Window and Its Applications”, International Journal of Engineering and Technology (IJET), ISSN : 0975-4024 Vol 7 No 4 Aug-Sep 2015.

[12] Hrishi Rakshit and Muhammad Ahsan Ullah, “A Comparative Study on Window Functions for Designing Efficient FIR Filter”, The 9th International Forum on Strategic Technology (IFOST), October 21-23, 2014, Cox’s Bazar, Bangladesh.